

Boson peak in supercooled liquids: Time domain observations and mode coupling theory

Hu Cang, Jie Li, Hans C. Andersen, and M. D. Fayer^{a)}

Department of Chemistry, Stanford University, Stanford, California 94305

(Received 9 May 2005; accepted 20 June 2005; published online 16 August 2005)

Optical heterodyne-detected optical Kerr effect (OHD-OKE) experiments are presented for the supercooled liquid acetylsalicylic acid (aspirin - ASP). The ASP data and previously published OHD-OKE data on supercooled dibutylphthalate (DBP) display highly damped oscillations with a periods of ~ 2 ps as the temperature is reduced to and below the mode coupling theory (MCT) temperature T_C . The oscillations become more pronounced below T_C . The oscillations can be interpreted as the time domain signature of the boson peak. Recently a schematic MCT model, the Sjögren model, was used to describe the OHD-OKE data for a number of supercooled liquids by Götze and Sperl [W. Götze and M. Sperl, *Phys. Rev. E* **92**, 105701 (2004)], but the short-time and low-temperature behaviors were not addressed. Franosch *et al.* [T. Franosch, W. Gotze, M. R. Mayr, and A. P. Singh, *Phys. Rev. E* **55**, 3183 (1997)] found that the Sjögren model could describe the boson peak observed by depolarized light-scattering (DLS) experiments on glycerol. The OHD-OKE experiment measures a susceptibility that is a time domain equivalent of the spectrum measured in DLS. Here we present a detailed analysis of the ASP and DBP data over a broad range of times and temperatures using the Sjögren model. The MCT schematic model is able to describe the data very well at all temperatures and relevant time scales. The trajectory of MCT parameters that fit the high-temperature data (no short-time oscillations) when continued below T_C results in calculations that reproduce the oscillations seen in the data. The results indicate that increasing translational-rotational coupling is responsible for the appearance of the boson peak as the temperature approaches and drops below T_C . © 2005 American Institute of Physics. [DOI: 10.1063/1.2000235]

I. INTRODUCTION

Anomalous excitations have been observed in disordered systems at terahertz (THz) frequencies by light,¹ x-ray,² neutron,³ and Raman scatterings,⁴ and dielectric relaxation experiments.⁵ These THz peaks in the density of states are termed the “boson peak.”⁶ The boson peak has also been observed in the time domain as a highly damped oscillation at ~ 1 ps in optical heterodyne-detected optical Kerr effect (OHD-OKE) experiments.⁷ The boson peak observed in different experiments would seem to have different origins. Dielectric relaxation experiments, OHD-OKE experiments, and light and Raman scattering experiments probe orientational or librational motions. The boson peak in these experiments are observed at temperatures very near or below the mode coupling theory^{8–10} (MCT) temperature, T_C , which is generally $\sim 1.25T_g$, where T_g is the glass transition temperature. Neutron and x-ray scattering experiments are sensitive to density fluctuations. These latter experiments observe the boson peak in glasses. The two sets of experiments may be observing phenomena that are distinct in nature, that is, orientational dynamics versus translational dynamics, or the observations may be different manifestations of a single phenomenon. It is important to point out that on very short time scales, the time derivative of the polarizability-polarizability

correlation function measured in OHD-OKE and DSL experiments can contain contributions from “collision-induced effects” that are in part caused by density fluctuations.

The boson peak involves some type of “excess” vibrational excitations at THz frequencies found in and only in disordered systems. A number of models have been proposed to describe the boson peak, including the disordered oscillators model,^{11,12} theories based on characteristics of the potential-energy landscape,^{11,13} and a schematic mode coupling theory.^{14–17} The MCT model has been applied to a detailed analysis of dynamic light-scattering data on supercooled glycerol.¹⁵

The OHD-OKE method has been used in the study of supercooled liquids where it is capable of producing very high-quality data over a wide range of temperatures and a very broad range of times from subpicoseconds, to hundreds of nanoseconds.^{7,18–20} Because the OHD-OKE experiment measures the time derivative of the polarizability-polarizability correlation function,²¹ the boson peak appears as a distinct oscillation in the data rather than a broad spectral feature in frequency domain experiments. Therefore, the onset of the boson peak and its development as the temperature is lowered to and past T_C is quite apparent.

In this paper, new OHD-OKE experimental data on supercooled acetylsalicylic acid (aspirin, ASP) are presented. As the temperature is reduced below T_C , a single cycle of an oscillation develops, becomes more pronounced, and shifts

^{a)}Electronic mail: fayer@stanford.edu

to earlier time. This same behavior was previously observed in OHD-OKE data for supercooled dibutylphthalate (DBP).⁷ Both the ASP and the DBP data are analyzed using the MCT schematic model.^{14,15} It is shown that the MCT schematic model is capable of reproducing the data on all time scales at temperatures well above T_C , where there is no short-time oscillatory manifestation of the boson peak. By continuing the “trajectory” of the parameters to fit the data as T is lowered, the oscillation in the data appears and fits the short-time data very well at and below T_C . The schematic MCT model consists of a correlation function that represents the observable polarizability-polarizability correlation function, which is coupled to a correlation function that represents the density fluctuations. For both sets of data, the parameter that seems to dominate the appearance of the boson peak is the coupling of the observable correlation function to the density correlation function. As the temperature is reduced, the coupling increases, and the boson peak appears.

II. EXPERIMENTAL METHOD AND RESULTS

Optical heterodyne-detected optical Kerr effect spectroscopy^{19–22} was used to measure the orientational dynamics of supercooled ASP and previously DBP.⁷ A pump pulse creates a time-dependent optical anisotropy that is monitored via a heterodyne detected probe pulse with a variable time delay. The OHD-OKE experiment measures the time derivative of the polarizability-polarizability (orientational) correlation function. The Fourier transform of the OHD-OKE signal is directly related to data obtained from depolarized light scattering,^{23–25} but the time domain OHD-OKE experiment can provide a better signal-to-noise ratio over a broader range of times for experiments conducted on very fast to moderate time scales.

To observe the full range of the dynamics several sets of experiments were performed with different pulse lengths and delays. For times $t < 30$ ns, a mode-locked 5-kHz Ti:Sapphire laser/regenerative amplifier system was used ($\lambda = 800$ nm) for both pump and probe. As has been described in detail previously, the pulse length was adjusted by from 75 fs to 10 ps as the time scale of the measurement increased to improve the signal-to-noise ratio. The longer pulses produce more signal for the longer-time portions of the data. For the shortest times, precision stepper motor delay line was used. For intermediate times, a 10 ps pulse was used with a long delay line to obtain data from 100 ps to 30 ns. For even longer times, a continuous-wave (CW) diode laser was used as the probe, and a fast digitizer (1 ns per point) recorded the data. The scans taken over various time ranges overlapped substantially, permitting the data sets to be merged by adjusting only their relative amplitudes. Additional experimental details have been published.^{26,27}

Dust was removed from the samples by vacuum distillation. The samples were in optical cells attached to the cold finger of a constant flow cryostat. A resistance thermometer attached to the sample cell permitted the temperature to be measured to better than 0.1 K. The samples were allowed to equilibrate at each temperature prior to measurement.

Figure 1 displays a sampling of the temperature-

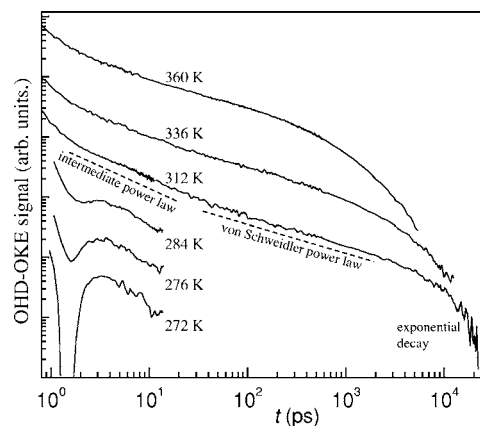


FIG. 1. Several OHD-OKE decay curves for supercooled acetylsalicylic acid (ASP). The data sets have been offset vertically for clarity. Above $T_C = 288$ K, the ASP data have the form observed previously for other supercooled liquids. The 312 K data has the various regions of the decay labeled. The dashed lines are aids to the eye indicating the power-law portions of the data. All data taken above T_C has the same functional form (see text). Below T_C the short-time portion of the data develops a highly damped oscillatory component.

dependent OHD-OKE data taken on ASP on a log plot. The data sets have been displaced along the vertical axis for clarity of presentation. More data and data for DBP are shown below in conjunction with the MCT analysis. Previous studies using OHD-OKE on five supercooled liquids, *ortho*-terphenyl, salol, benzophenone, 2-biphenylmethanol, and dibutylphthalate, demonstrate that they all display the same functional form for the decays well above T_C .^{19,20} ASP also has this functional form. The longest time scale portion of the data is an exponential decay, which is the final complete orientational randomization of the sample. This is termed the α relaxation.⁸ The α -relaxation decay time is highly temperature dependent, becoming increasingly long as the temperature is lowered. Immediately prior to the exponential decay is a power law, the von Schweidler power law,⁸ which reflects the onset of the α relaxation.⁸ The von Schweidler power-law exponent is temperature independent, but its amplitude varies with temperature.^{19,20} Both the exponential decay time constant and the von Schweidler power-law amplitude have been shown to obey the MCT scaling relationships.¹⁹ In Fig. 1, the exponential decay and the von Schweidler power law are indicated for the 312 K data.

On a shorter time scale than the von Schweidler power law is another power law, the “intermediate power law.” The intermediate power law has a temperature-independent exponent that is ~ 1 in the OHD-OKE data.¹⁹ Because the OHD-OKE experiments measure the time derivative of the orientational correlation function (polarizability-polarizability correlation function), the ~ 1 value for the exponent means that the correlation function decays approximately logarithmically. For temperatures above T_C , Götze and Sperl reproduced the intermediate power law in fitting OHD-OKE data using the schematic MCT model discussed below.¹⁷ On time scales shorter than the intermediate power law, there are very fast dynamics that are referred to as the fast β process.

The schematic MCT model of Götze and Sperl, which is based on the work of Sjögren,¹⁴ is able to reproduce the

observed experimental form of the data above T_C . For ASP, $T_C=288$ K. As can be seen in Fig. 1, as T is reduced below T_C , the short-time behavior of the data changes substantially. (The longer-time portions of the data are not shown at low temperature. They have the same form as the higher-temperature data, but the α relaxation becomes so slow that we are unable to follow it out to the end of the decay. As discussed in Sec. III, MCT cannot describe to long-time portion of the data below T_C .) As T is decreased below T_C , an oscillatory feature develops. The depth of the highly damped oscillation increases as the temperature is decreased. Because the OHD-OKE signal is heterodyne detected, the signal is measured at the polarization level. Therefore, the signal can go negative. The 272-K data do go negative, and the negative portion cannot be displayed on a log plot. In Sec. III, the schematic MCT model used to analyze the data is presented and applied to both the full set of ASP data and the DBP data.

III. SCHEMATIC MODE COUPLING THEORY MODEL AND DATA ANALYSIS

The OHD-OKE data can be described quantitatively by a schematic mode coupling model, as we shall now discuss. The mathematical form of the model was originally constructed by Sjögren¹⁴ to describe tagged particle dynamics in a liquid, but the same form was used by Franosch *et al.*¹⁵ to describe depolarized light scattering by glycerol, by Götze and Mayr¹⁶ to describe the boson peak in a glass at very low temperatures, by Götze and Voigtman²⁸ to describe various spectroscopies for supercooled propylene carbonate, and by Götze and Sperl¹⁷ to describe the OHD-OKE data for several molecular liquids above T_C . This model can be regarded as a generic model for an observable correlation function whose dynamics are coupled to a set of density degrees of freedom that undergo structural arrest as predicted by mode coupling theory. (Other schematic mode coupling models have also been used to address similar problems.^{29,30})

In the Sjögren's model, there are two correlation functions: $\phi_1(t)$ associated with density fluctuations and $\phi_2(t)$ which is the observable correlation function (in the present case the autocorrelation function of the polarizability anisotropy). The correlation functions obey the Mori-Zwanzig equations,

$$\ddot{\phi}_i(t) + \mu_i \dot{\phi}_i(t) + \Omega_i^2 \phi_i(t) + \Omega_i^2 \int_0^t d\tau m_i(t-\tau) \phi_i(\tau) = 0, \quad (1)$$

$i = 1, 2$

where the memory function kernels are

$$m_1(t) = \nu_1 \phi_1(t) + \nu_2 \phi_1^2(t), \quad (2)$$

$$m_2(t) = \kappa \phi_1(t) \phi_2(t). \quad (3)$$

The first correlator is an F_{12} MCT schematic model for the density fluctuations. It can undergo a type- B transition for the appropriate values of the parameters ν_1 and ν_2 . The F_{12} model can display the variety of type- B exponent parameters that are possible for a general mode coupling kinetic theory

of density fluctuations, and so this single correlator is a convenient simple model for density fluctuations. The second correlator has short-time damped harmonic oscillator behavior governed by μ_2 and Ω_2 and its coupling to the density correlator via the parameter κ largely determines its long-time behavior.

A feature observed in several supercooled molecular liquids is the approximately logarithmic decay of the correlation function, or approximately t^{-1} dependence of the OHD-OKE observable, at intermediate times in supercooled liquids above T_C (see Fig. 1, the intermediate power law).¹⁹ This behavior is observed for ASP as shown in Fig. 1 and in DBP.^{7,19} Previous work by Götze and Sperl¹⁷ has shown that this behavior arises in the Sjögren model provided the coupling parameter κ , which is a measure of the effect of density fluctuations on orientational relaxation (polarizability auto-correlation function), is large and increases as the temperature is lowered. As shown below, the same model with a large value of κ predicts the existence of highly damped oscillations in the orientational correlation function.

The experimental data for ASP and DBP were fitted with the schematic mode coupling model defined by Eqs. (1)–(3) using a downhill simplex algorithm. The MCT schematic model predicts the freezing of all relaxations at and below T_C , which is a well-known drawback of standard MCT. For data above the T_C , the entire decay starting from ~ 1 ps through the α -relaxation regime is fit to the model. Because MCT predicts that the long-time portion of the correlation function will approach an infinitely slow decay as T_C is approached from above, the theory does not correctly describe the slow component of the decay near T_C . For data taken at temperatures very close to and below T_C , only the short-time portion, from ~ 1 –15 ps is fitted. Because the number of parameters in the theory is large and each is in principle temperature dependent, we adopted the following procedure. The microscopic frequencies Ω_1 and Ω_2 were chosen to be independent of temperature. (The values that are necessary to fit the short-time oscillations are smaller than those reported by Götze and Sperl.¹⁷) As discussed further below, two damping constants μ_1 and μ_2 , which are also crucial for fitting the short-time oscillations, were varied. μ_1 was constrained to have values that varied relatively smoothly with temperature. μ_2 was found to be independent of temperature for ASP and to be almost independent of temperature for DBP. The mode coupling parameters ν_1 and ν_2 , and κ were freely varied for temperature well above T_C . As discussed further below, at and below T_C the ν_1 – ν_2 trajectory was extended along its high-temperature trajectory.

Figure 2(a) displays on a log plot the decays of the OHD-OKE signals of ASP (solid lines) and the fits to the data (dashed lines) using the Sjögren mode coupling schematic model described above. Fourteen of the 27 data sets that were measured for ASP are shown. The temperatures are given in the figure caption. At the higher temperatures, the data are shown for times between about 0.9 ps and 20 ns. At the lower temperatures, the data have a similar long-time appearance, but only the portions of the data fit with the model are shown. As T_C is approached from above, the boson peak oscillation develops. Below T_C it becomes very

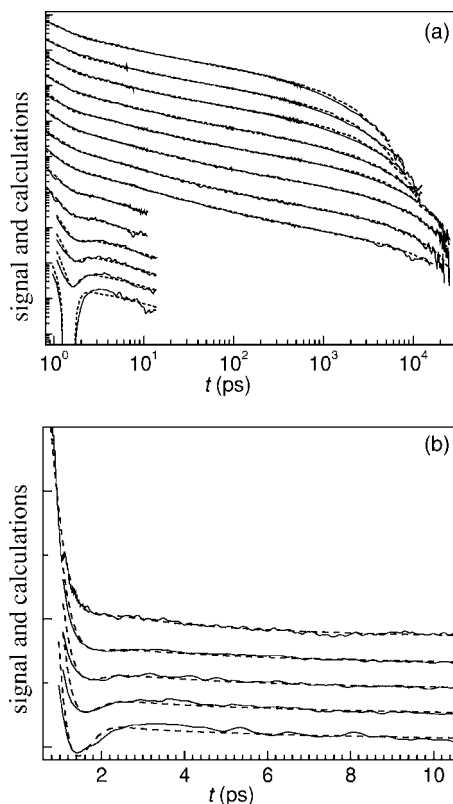


FIG. 2. (a) ASP OHD-OKE data (solid lines) and mode coupling schematic model fit to the data (dashed lines) at various temperatures (top to bottom: 360, 352, 344, 336, 328, 320, 312, 304, 296, 288, 284, 280, 276, and 272 K) on a log plot. The data are offset vertically for clarity of presentation. (b) The short-time portions of the data (solid lines) and fits (dashed lines) on a linear plot at the lowest five temperatures.

pronounced. At the lowest temperature, the signal goes negative at its minimum and cannot be displayed on a log plot. As can be seen in Fig. 2(a), the MCT schematic model reproduces the decay of OHD-OKE signal remarkably well. At the higher temperatures, the model reproduces the full time range of the data. Near and below T_C , the model accurately reproduces the onset and the development of the boson peak as the temperature is lowered. Figure 2(b) displays the short-time portion of the data at the lowest five temperatures and the fits to the data on a linear plot.

Figure 3 displays the trajectories of the key parameters used in fitting the ASP data. Figure 3(a) shows the trajectory of the values of ν_1 and ν_2 in Eq. (2). The circles correspond to the data at the 14 temperatures displayed in Fig. 2(a). The $\phi_1(t)$ density correlator, on cooling, undergoes an ergodic-nonergodic type-*B* transition when the values of ν_1 and ν_2 in Eq. (2) cross the solid curve shown in Fig. 3(a). The point at which the trajectory crosses the solid curve determines the value of the von Schweidler power-law exponent. The crossing point was fixed to reproduce the experimentally observed von Schweidler exponent for ASP. At high temperatures, the data could be fit with the value of ν_1 essentially constant and ν_2 increasing. However, as the temperature approaches T_C , simple MCT predicts that the longest time scale dynamics become too slow. The MCT prediction is that the longest time scale dynamics become infinitely slow at T_C , in contrast to experiment. The data can still be fit, but it is necessary to

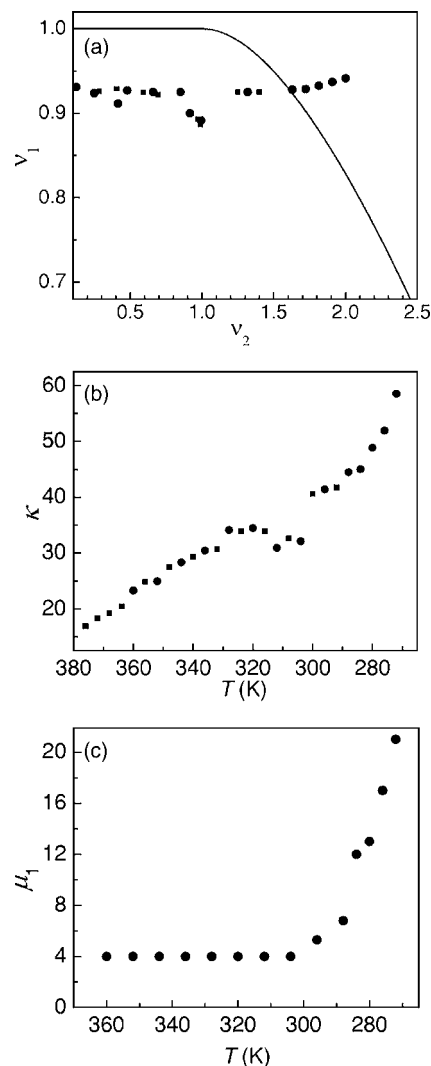


FIG. 3. (a) The trajectory of the ν_1 and ν_2 coefficients [Eq. (2)]. The circles correspond to the temperatures shown in Fig. 2(a). The solid curve defines the boundary for the ergodic-nonergodic type-*B* transition. The system is ergodic at high temperatures, to the left of and below the solid line. (b) The coupling constant κ [Eq. (3)] plotted vs T . The circles correspond to the temperatures shown in Fig. 2(a). κ determines the magnitude of the influence of the density correlator ϕ_1 on the observable orientational correlator, ϕ_2 . (c) The damping constant μ_1 [Eq. (1)] vs T .

significantly reduce the ν_1 value. This is an artifact that occurs at $\nu_2 \approx 1$. Therefore, for lower temperatures, the high-temperature trajectory was extended to intersect the solid curve to reproduce the von Schweidler exponent. Below T_C , the trajectory curves up slightly. This should not be taken to be significant. By varying the other parameters, it would be possible to stay on the high-temperature trajectory and still have excellent fits to the data below T_C .

The influence of the density degrees of freedom on the observable correlator $\phi_2(t)$ is determined by the value of κ in Eq. (3). κ is plotted vs T in Fig. 3(b). κ increases as the temperature is lowered. However, for the fits that used the points off of the high-temperature ν_1 - ν_2 trajectory [Fig. 3(a)], the κ values fall low. When the ν_1 - ν_2 trajectory is forced back onto the high-temperature path, κ continues its monotonic increase with decreasing temperature. The value

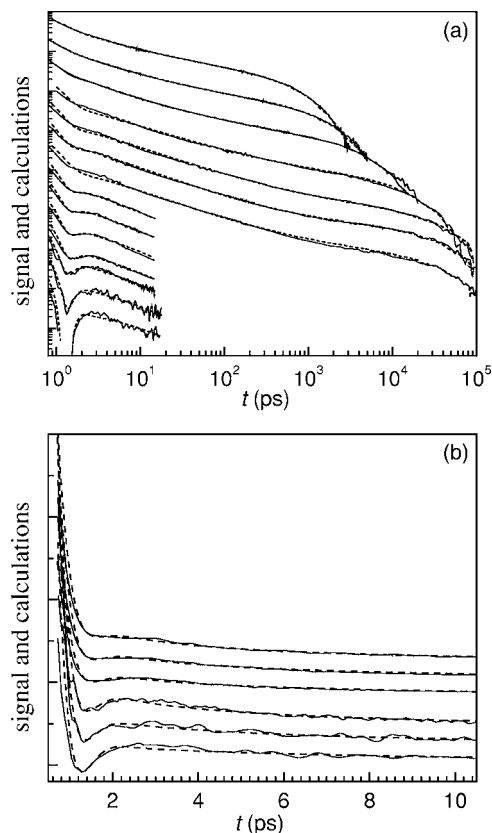


FIG. 4. (a) DBP OHD-OKE data (solid lines) and mode coupling schematic model fit to the data (dashed lines) at various temperatures (top to bottom: 290, 275, 260, 245, 238, 234, 230, 226, 223, 220, 217, 215, 210, and 205 K) on a log plot. The data are offset vertically for clarity of presentation. (b) The short-time portions of the data (solid lines) and fits (dashed lines) on a linear plot at the lowest six temperatures.

of the damping parameter, μ_1 is plotted in Fig. 3(c). $\mu_2 = 5.5$ at all temperatures. μ_1 is constant at high temperature, but increases rapidly near and below T_C .

Figure 4(a) displays on a log plot the decays of the OHD-OKE signals of DBP (solid lines) and the fits to the data (dashed lines). The temperatures are given in the figure caption. As with the ASP data, the fits are very good. At high temperatures, the entire range of the data is fit. Near and below $T_C = 227$ K, the fits accurately reproduce the onset and development of the boson peak. Figure 4(b) shows the data for the lowest six temperatures on a linear plot.

Figure 5 displays the trajectories of the key parameters used in fitting the DBP data. Figure 5(a) shows the trajectory of the values of ν_1 and ν_2 in Eq. (2). As in Fig 3(a), the solid curve shows the boundary for the ergodic-nonergodic type-B transition. The point at which the trajectory crosses the solid curve determines the value of the von Schweidler power-law exponent. The crossing point was fixed to reproduce the experimentally observed von Schweidler exponent for DBP. As with ASP, the higher-temperature points fall approximately on a line. As T_C is approached, to fit the long-time portion of the curve, the $\nu_1 - \nu_2$ points fall off of the high-temperature trajectory. Therefore, the high-temperature trajectory was extended to cross the solid curve at the point that yields the experimentally determined value of the von Schweidler power-law exponent. The points corresponding to tempera-

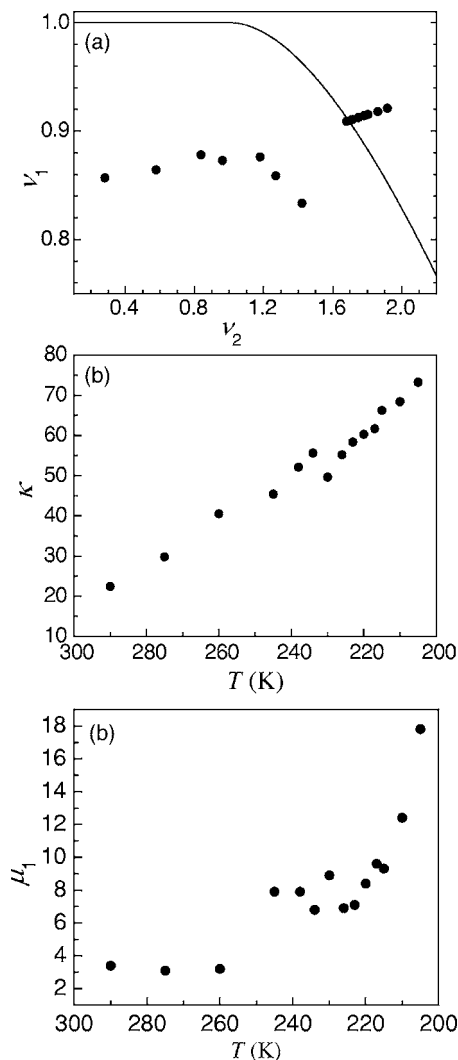


FIG. 5. (a) The trajectory of the ν_1 and ν_2 coefficients (Eq. (2)). The solid curve defines the boundary for the ergodic-nonergodic type-B transition. The system is ergodic at high temperatures, to the left of and below the solid line. (b) The coupling constant κ [Eq. (3)] plotted vs T . κ determines the magnitude of the influence of the density correlator ϕ_1 on the observable orientational correlator, ϕ_2 . (c) The damping constant μ_1 [Eq. (1)] vs T .

tures at and below T_C (on and to the right of the solid curve) were required to fall on the high-temperature trajectory in the fits. κ is plotted vs T in Fig. 5(b). As with ASP, κ increases as the temperature is lowered. The value of the damping parameter μ_1 is plotted in Fig. 3(c). μ_1 is relatively constant at high temperature; it increases rapidly near and below T_C . However, in contrast to ASP, there is more scatter in the points. This scatter is not significant. $\mu_2 = 6.1$ at high temperature but varies somewhat near T_C , taking on a maximum value of 6.9. Like the scatter in μ_1 , this variation is not significant. The main features are similar to ASP. μ_1 increases substantially at low temperature and μ_2 is essentially constant.

Figure 6 displays the two correlators $\phi_1(t)$ (density) and $\phi_2(t)$ (orientation) obtained from fitting the DBP data. A “well” (indicated by the arrow in Fig. 6) appears at ~ 1 to 2 ps in $\phi_2(t)$. The well corresponds to the boson peak. The OHD-OKE measures the time derivative of the correlation function. The time derivative gives rise to the oscillation in OHD-OKE signal. For the values of the parameters that gave

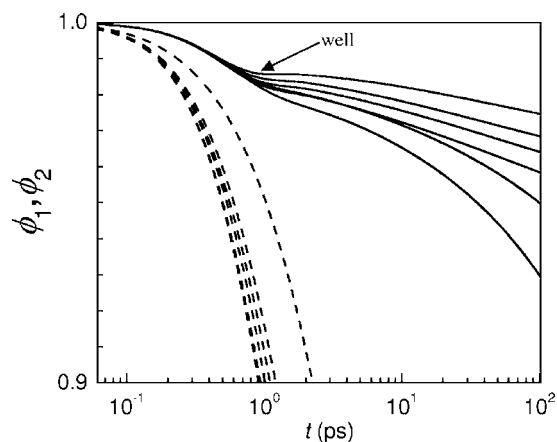


FIG. 6. The two correlators ϕ_1 (density, dashed) and ϕ_2 (orientation, solid) obtained from the fits to the OHD-OKE data of DBP. The curves are calculated for the temperatures (top to bottom) 205, 215, 220, 226, 234, and 245 K. Notice the “well” at ~ 1 to 2 ps in ϕ_2 (indicated by the arrow) that corresponds to the boson peak.

good fits to the experimental data, the density correlator $\phi_1(t)$ does not oscillate in this temperature range. The mathematical origin of the oscillatory behavior of $\phi_2(t)$ is thus not related to the oscillations in the density but rather is a consequence of strong coupling of the polarizability correlator to the nonoscillatory density correlator. The tiny well in ϕ_2 is the signature of the boson peak. It could easily be missed in a frequency domain spectrum, which may explain why most experiments report the observations of boson peak at temperatures much lower than T_C .

This use of the Sjögren’s model to fit the data makes no assumptions about the molecular origins of the polarizability anisotropy whose autocorrelation function is $\phi_2(t)$. Molecular orientation of the rigid parts of the molecules presumably plays an important role, but neither of the molecules studied is completely rigid and hence intramolecular conformational degrees of freedom can also affect the polarizability. There is also the possibility of collision-induced contributions to the polarizability anisotropy. The only assumptions made in applying the model are that the polarizability anisotropy is a dynamical variable that behaves as a damped harmonic oscillator whose dynamics is coupled to the density of the fluid in the manner described by the schematic mode coupling theory. The frequency and damping constants of this oscillator are parameters in the theory, as is the strength of the coupling of the anisotropy to the density. The detailed time dependence of the polarizability anisotropy correlation function then follows from that of the density autocorrelation function, which has been modeled with a schematic F_{12} model. Presumably the oscillations consist primarily of librational motion of the rigid portion of the molecule. Note that the OHD-OKE signal is the negative of the derivative of $\phi_2(t)$. Thus, on cooling, $\phi_2(t)$ itself starts to have oscillatory behavior (i.e., its derivative changes sign) about 15° – 20° below T_C . However, the oscillations in the derivative of $\phi_2(t)$ are noticeable at temperatures just below and very close to T_C .

IV. CONCLUDING REMARKS

We have presented the new OHD-OKE data for supercooled ASP and have analyzed the ASP data and previously reported DBP data in the vicinity of the mode coupling transition temperature. For both of these liquids, there is a highly damped oscillation in the observable that can be regarded as a high-temperature manifestation of the boson peak. The data can be well explained by the Sjögren’s MCT schematic model. The theory explains the boson peak oscillations as a damped oscillation of the polarizability anisotropy, which is presumably primarily a damped librational motion of molecules trapped in their cages for temperatures near and below the mode coupling temperature T_C . It has been noticed before that a strong coupling could “renormalize” the oscillation frequency Ω .¹⁵ Since the strong coupling is responsible for the nearly logarithmic decay observed in OHD-OKE experiment at temperatures higher and close to T_C ,¹⁷ it is puzzling why the oscillation is missing in some experiments at the same temperatures. Here the “missing” oscillation is found. Schematic MCT successfully describes both the boson peak and nearly logarithmic decay of the orientational correlation function that manifests itself as the intermediate power law in the OHD-OKE experiments. The schematic MCT is capable of fitting the data at each temperature, but it does not predict the temperature at which the oscillations appear. On cooling, for both liquids, the oscillations appear very close to the mode coupling T_C . This is consistent with the predictions of two theories^{11,13} based on the characteristics of the potential-energy landscape for a liquid.

ACKNOWLEDGMENTS

The authors thank M. Sperl and M. Letz for valuable discussions pertaining to this work. We are also grateful to M. Sperl for providing the algorithms used in the numerical evaluation of the theory. Three of the authors (H.C., J.L., and M.D.F.) thank the NSF (DMR-0322691), and another author (H.C.A.) thanks the NSF (CHE-0010117 and CHE-0408786) for support of this research.

¹N. V. Surovtsev, S. V. Adichtchev, E. Rössler, and M. A. Ramos, *J. Phys.: Condens. Matter* **16**, 223 (2004).

²B. Ruffe, M. Foret, M. Courtens, R. Vacher, and G. Monaco, *Phys. Rev. Lett.* **53**, 2316 (2003).

³U. Buegenau, N. Nücker, and A. J. Dianoux, *Phys. Rev. Lett.* **53**, 2316 (1984).

⁴N. J. Tao, G. Li, X. Chen, W. M. Du, and H. Z. Cummins, *Phys. Rev. A* **44**, 6665 (1991).

⁵P. Lunkenheimer, U. Schneider, R. Brand, and A. Loidl, *J. Contemp. Phys.* **41**, 15 (2000).

⁶C. A. Angell, Y. Yue, L.-M. Wang, J. R. D. Copley, S. Borick, and S. Mossa, *J. Phys.: Condens. Matter* **15**, 1051 (2003).

⁷D. D. Brace, S. D. Gottke, H. Cang, and M. D. Fayer, *J. Chem. Phys.* **116**, 1598 (2002).

⁸W. Götz, in *Liquids, Freezing and Glass Transition*, edited by D. L. J. P. Hansen and J. Zinn-Justin (North-Holland, Amsterdam, 1991).

⁹J.-P. Bouchaud and M. Mezard, *Prog. Theor. Phys. Suppl.* **126**, 181 (1997).

¹⁰J.-P. Bouchaud, L. Cugliandolo, J. Kurchan, and M. Mezard, *Physica A* **226**, 243 (1996).

¹¹T. S. Grigera, V. Martin-Mayor, G. Parisi, and P. Verrocchio, *Nature (London)* **422**, 289 (2003).

¹²W. Schirmacher, G. Diesemann, and C. Ganter, *Phys. Rev. Lett.* **81**, 136 (1998).

- ¹³V. Lubchenko and P. G. Wolynes, Proc. Natl. Acad. Sci. U.S.A. **100**, 1515 (2003).
- ¹⁴L. Sjögren, Phys. Rev. A **33**, 1254 (1986).
- ¹⁵T. Franosch, W. Götze, M. R. Mayr, and A. P. Singh, Phys. Rev. E **55**, 3183 (1997).
- ¹⁶W. Götze and M. R. Mayr, Phys. Rev. E **61**, 587 (2000).
- ¹⁷W. Götze and M. Sperl, Phys. Rev. Lett. **92**, 105701 (2004).
- ¹⁸G. Hinze, D. D. Brace, S. D. Gottke, and M. D. Fayer, Phys. Rev. Lett. **84**, 2437 (2000).
- ¹⁹H. Cang, V. N. Novikov, and M. D. Fayer, J. Chem. Phys. **118**, 2800 (2003).
- ²⁰H. Cang, V. N. Novikov, and M. D. Fayer, Phys. Rev. Lett. **90**, 197401 (2003).
- ²¹D. McMorrow, W. T. Lotshaw, and G. Kenney-Wallace, IEEE J. Quantum Electron. **24**, 443 (1988).
- ²²G. Hinze, D. D. Brace, S. D. Gottke, and M. D. Fayer, J. Chem. Phys. **113**, 3723 (2000).
- ²³Y. Kai, S. Kinoshita, M. Yamaguchi, and T. Yagi, J. Mol. Liq. **65–66**, 413 (1995).
- ²⁴Y. X. Yan and K. A. Nelson, J. Chem. Phys. **87**, 6240 (1987).
- ²⁵F. W. Deeg, J. J. Stankus, S. R. Greenfield, V. J. Newell, and M. D. Fayer, J. Chem. Phys. **90**, 6893 (1989).
- ²⁶S. D. Gottke, G. Hinze, D. D. Brace, and M. D. Fayer, J. Phys. Chem. B **105**, 238 (2001).
- ²⁷S. D. Gottke, D. D. Brace, H. Cang, and M. D. Fayer, J. Chem. Phys. **116**, 360 (2002).
- ²⁸W. Götze and T. Voigtmann, Phys. Rev. E **61**, 4133 (2000).
- ²⁹C. Alba-siminoesco and M. Krauzman, J. Chem. Phys. **102**, 5674 (1995).
- ³⁰S. P. Das, Phys. Rev. E **59**, 3870 (1999).